

MULTI-FUNCTIONAL K_{IC} -TEST SPECIMEN FOR THE ASSESSMENT OF DIFFERENT TOOL- AND HIGH-SPEED-STEEL PROPERTIES

VEČFUNKCIJSKI K_{IC} -PREIZKUŠANEC ZA DOLOČANJE RAZLIČNIH LASTNOSTI ORODNIH IN HITROREZNIH JEKEL

Vojteh Leskovšek, Bojan Podgornik

Institute of Metals and Technology, Lepi pot 11, 1000 Ljubljana, Slovenia
vojteh.leskovsek@imt.si

Prejem rokopisa – received: 2013-01-31; sprejem za objavo – accepted for publication: 2013-04-02

Depending on the differences in the balanced alloy composition and steel processing technology, the properties of tool and high-speed steel, like temper resistance, hot yield strength, ductility and toughness, thermal fatigue and shock resistance, as well as wear resistance can differ considerably among the same type of steel. A high hot-yield strength, a high temper resistance and a good ductility tend to result in a high resistance to thermal fatigue, while a resistance to mechanical and thermal shocks depends on the ductility and toughness. However, the properties of tool and high-speed steels also depend on the final vacuum-heat-treatment process. Normally, hardness and fracture toughness are used to determine the influence of vacuum-heat-treatment parameters and to optimize them for the specific operating conditions of the tool. However, there are also other tool properties which are equally important and need to be taken into consideration. To determine such a wide range of properties, different test procedures and different test specimens are required since none of the standard tests alone is capable of providing the relevant properties completely. Currently the best overall appraisal of tool and high-speed steel applicability seems to be a combination of fracture toughness, bending or compression testing and in specific cases of impact or small-punch creep tests. The aim of the paper is to show the possibility of using a single K_{IC} -test specimen for the determination of such a wide range of properties, being important for tool and high-speed steels. Besides that, the usability of K_{IC} -test specimens for the assessment of technological properties such as nitridability, machinability, wear resistance, etc. was confirmed.

Keywords: tool steel, vacuum heat treatment, characterization, fracture toughness

Ovisno od razlik v sestavi in tehnologije izdelave jekla lahko pri isti vrsti orodnega ali hitroreznega jekla močno variirajo lastnosti, kot so: odpornost proti popuščenju, natezna trdnost v vročem, duktilnost in žilavost, odpornost proti termičnemu utrujanju in udarcem, kot tudi odpornost proti obrabi. Visoka meja elastičnosti v vročem, velika odpornost proti popuščenju in dobra duktilnost se izražajo v visoki odpornosti proti termičnemu utrujanju, medtem ko sta odpornost proti mehanskim udarcem in termičnim šokom odvisni od duktilnosti in žilavosti. Vendar pa so lastnosti orodnega in hitroreznega jekla odvisne tudi od procesa končne vakuumske toplotne obdelave. Navadno se uporabljata trdota in lomna žilavost za ugotavljanje vpliva parametrov vakuumske toplotne obdelave in za njeno optimiranje pri orodjih, namenjenih specifičnim razmeram pri uporabi. Vendar obstajajo tudi druge lastnosti orodja, ki so enako pomembne in jih je potrebno upoštevati. Za določanje tako širokega področja lastnosti so potrebne različne vrste preizkusov in različni preizkusni vzorci, saj nobena standardna preizkusna metoda ni sposobna ugotavljanja vseh lastnosti. Trenutno najboljše presojanje uporabnosti orodnih in hitroreznih jekel omogoča kombinacija lomne žilavosti, upogibne ali tlačne trdnosti in v posebnih primerih udarni preizkus ali "small-punch" preizkus lezenja. Namen članka je prikazati možnost uporabe K_{IC} -preizkušanca za določanje različnih lastnosti, pomembnih za orodna in hitroreznega jekla. Poleg tega je bilo potrjeno, da K_{IC} -preizkusni vzorec omogoča tudi določanje tehnoloških lastnosti, kot so sposobnost za nitriranje, obdelovalnost in obrabna odpornost in druge.

Ključne besede: orodno jeklo, vakuumska toplotna obdelava, karakterizacija, lomna žilavost

1 INTRODUCTION

The forming industry is confronted with ever-increasing demands for higher productivity, lower production costs and more complex products, which together with an increased focus on advanced, high-strength, low-weight materials put increased requirements on tools and dies.¹⁻⁴ Consequently, this means strengthened property requirements for the tool and high-speed steels, including temper resistance, hot yield strength, ductility and toughness, wear resistance, thermal fatigue and shock resistance.^{5,6} Furthermore, with the tool design being pushed to the very limit of the material strength, any unexpected deterioration in the tool material properties will eventually lead to premature and unwanted tool failure. Therefore, tool and high-speed steels are conti-

nuously subjected to the development, both in the direction of improved properties as well as better quality with reduced properties' deviation.

Many of the tool- and high-speed-steel grades used today have been developed over a period of several decades. The most significant developments to date are the balanced chemical composition and the introduction of specific, technologically optimised production steps for an optimally annealed condition. Depending on the differences in the balanced alloy composition and the optimised processing route, the material properties can differ considerably among the same type of martensitic tool and high-speed steels. A high hot-yield strength, a high temper resistance and a good ductility tend to result in a high resistance to thermal fatigue. The resistance to mechanical and thermal shocks depends mainly on the

ductility and toughness, but to some extent it is also related to a high yield strength. Finally, the hardness and microstructure will define the friction, the wear and the anti-galling properties of the tool.

All the properties of tool and high-speed steels depend not only on the balanced chemical composition and the processing route, but also greatly on the final vacuum-heat-treatment process, which defines the final microstructure. Real metallic materials, i.e., tool steels, usually have a multi-phase microstructure with carbide precipitates and non-metallic inclusions. When the tools are subjected to loads, local stress concentrations will occur next to these hard, non-deformable, wear-resistant particles, which, if stresses cannot be released through micro-yielding of the matrix, will accelerate tool breakage.⁷⁻⁹ Traditionally, a trade-off between a tough matrix and hard, wear-resistant carbide precipitates was required. Vacuum heat treatment, on the other hand, allows the optimization of the tool-steel microstructure, which satisfies ever greater demands on the properties of tools and dies, particularly in respect of a greater fracture toughness, while maintaining or even increasing the hardness and wear resistance.¹⁰ In this respect the hardness and fracture toughness, K_{Ic} , were found to be the most suitable parameters when optimizing the final vacuum heat treatment of tool and high-speed steels.¹¹

Despite the enormous variety of tooling operations, some basic properties of tool materials are common to almost all applications. These properties are the ductility, toughness and hardness.^{8,10,12} Ductility and toughness prevent instantaneous fracture of the tool or tool edges due to local overload, while a high hardness prevents any local plastic deformation. However, ductility, toughness and hardness are more or less mutually exclusive properties, which means the prevention of instantaneous tool failure is often connected with a critical hardness level that must not be exceeded in a specific application. On the other hand, a low hardness may lead to a premature thermal shock, despite the associated high toughness level. Therefore, for a given hardness, the ductility and toughness of the tool should be as high as possible to ensure a good cracking resistance.¹⁰

Besides hardness, ductility and toughness there are also other tool steel properties that are becoming equally important as we move towards more and more complex tools. These include creep and wear resistance, bending strength, elastic properties under bending as well as compressive properties at room and elevated temperatures. Finally, the time and costs required to produce a tool depend on the technological properties, like high-speed machinability, grindability, nitridability, etc. Although all these properties can be determined using standard test methods, each one requires specific and often quite unique test specimens, which are expensive and not always easy to produce. Furthermore, different geometries of standard specimens mean different heat-treatment conditions, which makes it practically impossi-

ble to directly correlate the properties of tool and high-speed steels after the final heat treatment.

Therefore, the aim of this research work was to determine the applicability of a single K_{Ic} -test specimen for the determination of a very wide range of properties in the final heat-treated condition, which are important for tool and high-speed steels. Furthermore, work is intended to show the potential of K_{Ic} -test specimens for optimizing the final vacuum heat treatment of tool and high-speed steels.

2 RELEVANT TOOL STEEL PROPERTIES

2.1 Ductility, toughness and hardness

Ductility and toughness were found to be the most relevant properties in terms of the resistance to total failure of tool and high-speed steels, being a result of mechanical or thermal overloading.^{8,12} However, these are two different material properties, even though both are too often referred to as toughness since the opposite of both is brittleness. Unfortunately, no standardised tests for the determination of toughness or ductility are in common use and although some data are available, the use of different test methods leads to confusion. The importance of ductility and toughness for tool-steel performance depends a lot on the tool geometry.¹² In the case of smooth un-notched surfaces the ductility and the fracture stress are the relevant material properties. However, if sharp notches or cracks are present, which is more critical, the toughness is the most relevant property. From this point of view, tool and high-speed steels should be optimised in terms of ductility for the un-notched regions, and in terms of toughness for the notched regions.

The most reliable measure of toughness is the plain-strain fracture toughness. The same value of fracture toughness should be found for specimens of the same material but with different geometries and with a critical combination of crack size and shape and fracture stress. Within certain limits, this is indeed the case, and information about the fracture toughness can be used to predict the failure for different combinations of stress and crack size and for different geometries.¹³ Although standardized methods for a fracture-toughness determination are available,^{14,15} their applicability is limited in the case of hard and brittle materials, such as tool and high-speed steels.^{10,11,16} Due to the high notch sensitivity, the manufacture of a sharp fatigue crack is difficult and expensive. On the other hand, a method based on a circumferentially notched and fatigue-precracked tensile specimen^{17,18} (**Figure 1**) has been found to be the most promising alternative method.^{11,17,19} The fatigue crack in the specimen can be obtained without producing any disturbing effect on the fracture toughness of the steel if such a crack is obtained in the soft-annealed condition, i.e., prior to the final heat treatment.¹⁹

The advantage of the K_{Ic} -test specimen over the standardized CT specimen (ASTM E399-90) lies in the radial symmetry, which makes the specimen particularly suitable for studying the influence of the microstructure on the fracture toughness. The advantage relates to the heat transfer, which provides a completely uniform microstructure.^{19,20} Furthermore, in the case of K_{Ic} -test specimens the fatigue crack can be created with rotating-bending loading before the final heat treatment.^{11,19} And finally, for K_{Ic} -test specimens, plain-strain conditions can be achieved using specimens with smaller dimensions than those of conventional CT test specimens. Shen Wei et al.²¹ proved that for circumferentially notched and precracked round-bar tensile specimens, plain-strain conditions are achieved when $D \geq 1.5 (K_{Ic}/R_{p0.2})^2$ and $L \geq 4 \cdot D (R_{p0.2}$ is the yield stress).

In the case of circumferentially notched and fatigue-precracked tensile-test specimens showing linearly elastic behaviour up to fracture, the fracture toughness K_{Ic} can be calculated using equation (1)²²:

$$K_{Ic} = \frac{P}{\sqrt{D^3}} \left(-1.27 + 1.72 \frac{D}{d} \right) \quad (1)$$

where P is the load at failure, D is the outside non-notched diameter, and d is the diameter of the instantly fractured area, i.e., the diameter of the ligament next to the crack. Eqn. (1) is valid as long as the condition $0.5 < d/D < 0.8$ is fulfilled. It is known that the fracture toughness of conventionally produced tool steels depends on the specimen orientation.²³ It is the highest for crack propagation perpendicular to the rolling direction and the lowest for a crack propagating along the rolling direction. Therefore, the way how specimens are taken from the master block is very important and to be on the conservative side specimens should be taken in a short transverse direction.

Besides toughness also the hardness of tool and high-speed steels greatly depends on the vacuum-heat-

treatment procedure, with both properties being mutually related. The hardening mechanism is different for as-quenched and fully-heat-treated tool steels. In the as-quenched tool steel, mostly the work-hardening and solid-solution hardening affect the steel's hardness. Tempering then leads to the precipitation of carbide particles and a significant decrease of the carbon content in a solid solution of martensite as well as of the density of dislocations. Thus, the hardness of fully-heat-treated tool steels is mainly the result of precipitation hardening and, to a small extent, solid-solution hardening. A high hardness is required to facilitate a high resistance to plastic deformation and wear. However, with a high hardness the toughness is reduced, which can lead to cracking. Therefore, for a given hardness level, the fracture toughness of tool and high-speed steels should be as high as possible to ensure a good cracking resistance.

2.2 Bending strength

The standard bend testing, which is widely used to measure the bending fracture strength of tool and high-speed steels is considered to be the most reliable and to give a great deal of information regarding the toughness and the ductility of the material. According to the ASTM E290-09 standard,²⁴ bend testing can be performed under 3- or 4-point loading. The bending moment diagrams show that for each mode compression stress is present on the concave side of the specimen, which for the 4-point mode is constant in a central span between the two inner supports, the opposite to the peak concentration under the central support of the 3-point method. Stresses under bending can be calculated using simple conventional theory, but only if the stress throughout the specimen remains below the limit of proportionality. If the limit of proportionality is exceeded than the calculated stress will be higher than the actual stress, which in the extreme case of fully plastic deformation reaches 1.5 times the actual stress value.

Hoyle and Ineson²⁵ showed that by progressively correcting the calculated stress, taking into account the limit of proportionality, a curve similar to the tensile curves can be obtained. An analysis of such a corrected curve can provide data related to the toughness properties, and more important, the behaviour of tool and high-speed steels. By performing experiments in the elastic region of high-speed steel, it was found that the test can discriminate between the elastic behaviour of good and bad specimens.²⁵ This can be quantified by using an empirical relationship L/ϕ , the ratio of the actual limit of proportionality L to the fracture stress ϕ , taken at a given hardness. Another parameter obtained from the bending-test curve is the amount of plastic deformation, or more correctly the deformation beyond the limit of proportionality. This parameter is used to determine the energy to fracture. Finally, with bend testing the modulus of elasticity is also obtained.

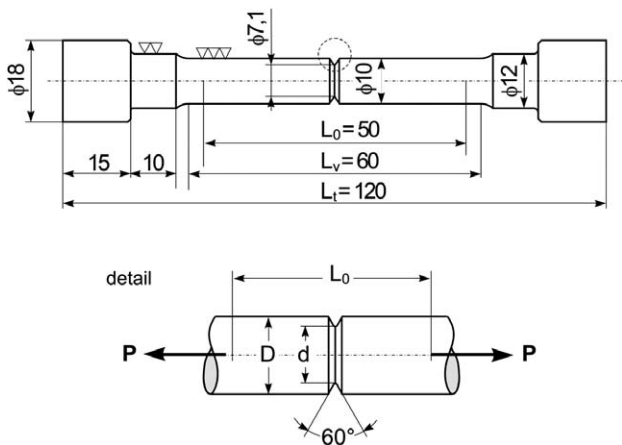


Figure 1: Circumferentially notched and fatigue-precracked K_{Ic} -test specimen (all dimensions are in millimeters)

Slika 1: K_{Ic} -preizkušavec z obodno zarezo in utrujenostno inicialno razpoko (vse dimenzije so v milimetrih)

2.3 Compression properties

For tool and high-speed steels in the hardened and tempered condition the compression properties are considered to be of far greater importance than the tensile properties. Namely, their ductility in the hardened and tempered condition is low and therefore not easily revealed in a tensile test. The compression properties of tool and high-speed steels at room and elevated temperatures can be determined using standard test methods ASTM E9-09²⁶ and ASTM E209,²⁷ respectively. The parameters obtained from the compression test include the compressive strength, the compressive yield strength and the strain-hardening exponent. Compressive strength correlates with the hardness of tool steel, while the strain-hardening exponent describes its ductility.

2.4 High-speed machinability

The trend among toolmakers is to abandon the old strategy of roughing and machining a piece of steel, hardening it, finishing and grinding it, eroding features impossible to cut, and polishing the surfaces. With the introduction of high spindle-speed machines, which can create an excellent surface finish that needs little or no polishing, toolmakers prefer high-speed machining (HSM) in hardened conditions. In the case of HSM complex tool geometries can be machined in a single operation, thus eliminating many time-consuming operations and reducing costs. Since HSM combines the roughing, semi-finishing, and finishing operations of hardened steel, spindles with high speed to allow fine step-overs for finishing and with an adequate amount of torque for roughing are required. Today, the HSM of hardened and tempered tool and high-speed steels with an uninterrupted cut is possible up to a hardness of about 65–67 HRC.²⁸

HSM is different from conventional machining and to make it work a completely new philosophy needs to be adopted.²⁹ The understanding begins with the definition of high-speed machining. Rather than using the conventional definitions based on spindle speed, tool-tip speed, or bearing ratio, it has to be defined in terms of frequency. According to this, HSM occurs as the tooth-pass frequency approaches a substantial fraction of the dominant natural frequency of the machine-tool system.²⁹ A definition based on tool-pass frequency gives engineers a tool for eliminating chatter and its deteriorating effect on tool wear, surface finish, and machine life. Machinability as well as the HSM of different tool and high-speed steels can vary considerably. Factors largely influencing the machinability of tool steels are the chemical composition, the microstructure, the hardness, non-metallic inclusions and residual stresses. However, the main factor generally regarded as influencing the machinability of a tool steel is its hardness. The harder the material is and the more carbides it has the more difficult it is to machine.

2.5 Grindability

As grinding is an important operation in the final production of many components from tool and high-speed steel, the grindability of the material in the hardened and tempered condition can have important consequences for productivity and economics. Tool and high-speed steels have a high hardness and wear resistance, which makes them difficult to grind, especially when using aluminium-oxide wheels. Furthermore, high temperatures generated during the grinding of tool and high-speed steels lead to thermal damage in the form of surface oxidation, softening, tensile residual stress generation and re-hardening.³⁰ Therefore, one needs to differentiate between thermal sensitivity, a material's tendency to be damaged at high temperatures, and grindability, the material's effect on the cutting ability of the abrasive grits.³¹

Hardened and tempered tool and high-speed steels are composed of tungsten-molybdenum carbides (≈ 1400 HV) and vanadium carbides (≈ 3300 HV) in a matrix of martensitic steel. It was found that the vanadium content and the size of the vanadium carbides are the dominant factors affecting the grindability of high-speed steel.³² According to König and Messer³³ grindability can be expressed by the G-factor, i.e., the ratio of ground material volume to grinding wheel volume lost. By taking the equivalent carbide content (ECC), based on the stoichiometric sum of the carbide-forming elements in mass fractions w ($ECC/\% = w(W) + 1.9 \cdot w(Mo) + 6.3 \cdot w(V)$), it was shown that the G-ratio is decreasing with increased ECC.³³ When comparing conventional and powder metallurgy (P/M) tool steels the G-ratio for latter can be up to 7 times higher, thus indicating better grindability.³⁴ In this case better grindability is the result of a smaller carbide size found in the P/M steels.³²

Besides the G-ratio, being an adequate way to measure grindability, the rate of power increase represents a more meaningful measurement. Quantitatively, the machinability and grindability can be determined on the basis of a tribological evaluation as well as by measuring the forces during cutting or grinding.³⁵ Thus, the instrumented wedge grinding test (WGT),³⁶ involving the measurement of grinding forces in the tangential and radial directions as well as the contact zone temperature, gives the capability of characterizing the material behaviour resulting from the grinding operation.

3 EXPERIMENTAL

3.1 Material and vacuum heat treatment

To demonstrate the applicability and potential of K_{Ic} -test specimens (**Figure 1**), ESR high-speed steel AISI M2 (delivered in the shape of rolled, soft-annealed and peeled bars $\phi 20$ mm \times 4000 mm) with the following chemical composition (mass fractions): 0.89 % C, 0.20 % Si, 0.26 % Mn, 0.027 % P, 0.001 % S, 3.91 % Cr, 4.74 %

Table 1: Tempering temperatures used in the vacuum furnace**Tabela 1:** Temperature popuščanja v vakuumski peči

Tempering temperature (°C)	500	520	540	550	555	560	580	600	630
K_{Ic} -test specimens group A $T_A = 1180$ °C	A1	A2	A3	A4	–	–	A7	A8	A9
K_{Ic} -test specimens group B $T_A = 1230$ °C	B1	B2	B3	B4	B5	B6	B7	B8	B9

Mo, 1.74 % V, and 6.10 % W was used. K_{Ic} -test specimens were cut from the delivered bars in the direction of rolling and due to the high notch sensitivity of the hardened high-speed steel, a fatigue pre-crack of about 0.3 mm was created prior to the final heat treatment using a rotating-bending loading. All the K_{Ic} -test specimens were then quenched in a horizontal vacuum furnace, using N_2 at a pressure of 5 bar. After the last preheat the specimens were rapidly heated (25 °C/min) to the austenitizing temperature of 1180 °C or 1230 °C, soaked for 2 min and then gas quenched to a temperature of 80 °C. Finally, high-pressure, gas-quenched K_{Ic} -test specimens were double tempered for 1 h, which was carried out in the same furnace at 9 different tempering temperatures (**Table 1**). For each tempering temperature at least 16 K_{Ic} -test specimens were prepared.

3.2 Material properties evaluation

The fracture-toughness measurement on the K_{Ic} -test specimens was performed at room temperature using an Instron 1255 tensile-test machine and a special specimen fixture, which provided complete axiality of the tensile load. The cross-head speed was 1.0 mm/min, the speed used for standard tensile-test specimens. During each tensile test the tensile-load/displacement relationship until failure was recorded, which for all K_{Ic} -test specimens investigated showed linearly elastic behaviour, thus confirming the validity of Eqn. (1).

After the tensile test the notch-section diameter d and the radial distance of the crack initiation site from the fatigue crack frontline x were measured for each fractured surface using an optical microscope. The analysis of the fractured surfaces was followed by a Rockwell-C hardness (HRC) measurement, performed on each half of the individual K_{Ic} -test specimen using a Wilson 4JR hardness machine.

One half of the fractured K_{Ic} -test specimen was then used to make a cylindrical 4-point bending-test specimen ($\phi 5$ mm \times 60 mm), with the bending test carried out according to the ASTM E290-09 standard.²⁴ The 4-point bending-test specimens were prepared by high-speed turning, using Sandvik SNMG 120408 K15 cutting inserts, a feed rate of 0.1 mm/r, a depth of cut of 0.15 mm and a cutting speed of 100 m/min.²⁸ After high-speed turning, cylindrical specimens were further ground by high-speed, centreless grinding (HSCG, $v_g = 63$ m/s) in order to obtain the prescribed average surface roughness of 0.2 μ m. During the preparation of the 4-point

bending-test specimens, high-speed turning and grinding procedures were also used to evaluate the high-speed machinability and grindability of the investigated high-speed steel. The high-speed machinability was analysed in terms of the evolution of the cutting inserts' flank and the notch wear and appearance of the chips. On the other hand, the effectiveness of the grinding and grindability were assessed on the basis of the final surface roughness, achieved on 4-point bending-test specimens. In spite of the fact that the G-ratio is normally used to measure the effectiveness of the grinding wheel, we rather focused on the quality of the ground surface.

The other half of the fractured K_{Ic} -test specimen was cut 6 mm below the fractured surface in order to prepare a metallographic sample for the fracture and microstructure examination. A further 12.5 mm down compression test specimen ($\phi 10$ mm \times 12.5 mm) was cut from the fractured K_{Ic} -test specimen and tested on an Instron 1255 test machine at room temperature according to the ASTM E9-09 standard.²⁶ The compression-test results included the compressive yield strength, the compressive strength, the modulus of elasticity and the strain-hardening exponent.

4 RESULTS

4.1 Fractography and metallography

Through an analysis of the fractured surface the main crack-nucleation site can be identified. As shown in **Figure 2a**, the main crack-nucleation site does not coincide with the fatigue crack frontline in the case of high-speed steels.¹¹ For all the investigated specimens the main crack-nucleation site was found to be slightly away from the fatigue crack, with typical Chevron lines designating the crack initiation and the direction of propagation. Furthermore, no crack re-initiation in the very tip of the existing fatigue crack could be observed. A higher magnification of the crack-nucleation site, denominated also as the weak spot, revealed the site to be composed of large carbide clusters and strings and a region of dimpled ductile fracture (**Figure 2b**).

The presence of the weak spot leads to an over estimation of the fracture toughness. Blunting of the fatigue-crack tip due to its branching out causes a constraint effect and displaces the region of maximum stresses and crack re-initiation from the area close to the surface more into the bulk, ahead of the fatigue-crack frontline.¹⁹ Consequently, the apparent fracture toughness is elevated. In such cases a statistical analysis of the

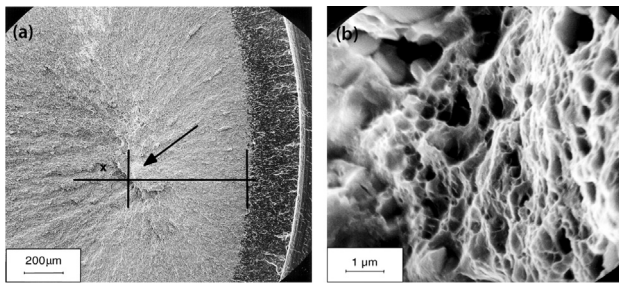


Figure 2: a) Typical fractured surface of a K_{Ic} -test specimen from high-speed steel and b) main crack-nucleation site

Slika 2: a) Značilna površina preloma K_{Ic} -preizkušanca iz hitrozreznega jekla in b) mesto nukleacije razpoke

measured fracture toughness vs. the position of the weak spot should be employed. If a linear correlation coefficient R is larger than 0.6 the fracture toughness obtained on a statistically relevant number of specimens (>10) is already the true value. Otherwise, a linear extrapolation to the fatigue-crack frontline (i.e., $x = 0$) should be performed.¹⁹ In the present case, for all specimen groups, the linear correlation coefficient R was between 0.8 and 0.95, thus confirming the validity of the measured fracture-toughness values.

Polishing the fractured surface and the preparation of metallographic specimens reveal the microstructure of the high-speed steel after a particular vacuum heat treatment. Microstructures for K_{Ic} -test specimens austenitized from 1230 °C and tempered at temperatures between 500 °C and 600 °C are shown in **Figure 3**. The microstructure of the investigated high-speed steel consists of tempered martensite, fairly well dispersed undissolved eutectic carbides and some stabilised retained austenite in the matrix. The amount of retained austenite is reduced with increased tempering temperature and becomes nearly absent above 580 °C. A lower austenitizing temperature of 1180 °C was found to produce a

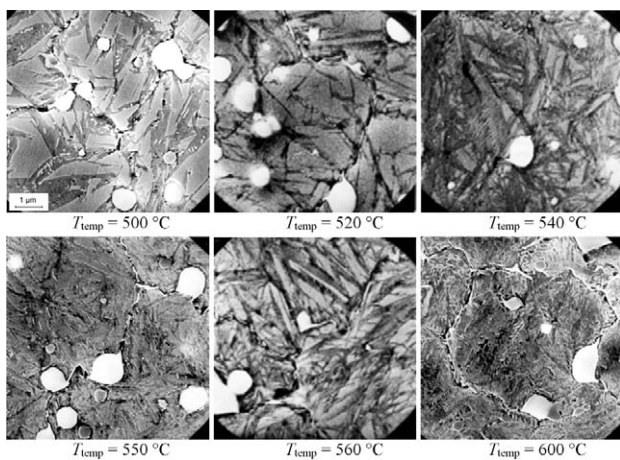


Figure 3: Typical microstructure of group B K_{Ic} -test specimens austenitized from 1230 °C

Slika 3: Značilna mikrostruktura skupine B K_{Ic} preizkušancev, avstentiziranih iz 1230 °C

similar microstructure. However, it resulted in a higher volume fraction of undissolved carbide particles, which can be up to three times higher. Quantitative metallography and microscopy, including Scanning Electron Microscopy with Electron Back-Scattered Diffraction (SEM/EBSD), further enable a detailed determination of the eutectic carbide type, size and volume fraction, the cumulative fraction of undissolved eutectic carbides and carbide clusters, and the volume fraction of retained austenite.

4.2 Fracture toughness and hardness

The fracture toughness and hardness values for two austenitizing temperatures are presented in the tempering diagram, shown in **Figure 4**. For both austenitizing temperatures the fracture toughness shows a peak value of more than 15 $\text{MPa m}^{1/2}$ at the lowest tempering temperature of 500 °C, which coincides with the relatively high volume fraction of stabilised retained austenite and the low hardness (60–61 HRC). By increasing the tempering temperature the hardness level of the investigated high-speed steel was increasing before reaching a peak value of 64–66 HRC between 560 °C and 570 °C, which was followed by a further decrease in the hardness. However, at about the same hardness, the under-tempered specimens quenched from the same austenitizing temperature, show a higher fracture-toughness value. For example, after vacuum quenching from 1230 °C and double tempering at about 620 °C the investigated high-speed steel achieves a hardness of 63 HRC and a fracture toughness of 8.5 $\text{MPa m}^{1/2}$. The same hardness, but with an approximately 30 % higher fracture toughness, can be obtained by using a tempering temperature of ≈ 510 °C (**Figure 4**). The use of a lower austenitizing temperature results in a reduced hardness and an increased fracture toughness, with the difference becoming more evident at higher tempering temperatures. These results clearly show that the high volume fraction of stabilized retained austenite in under-tempered high-speed steel significantly improves its fracture toughness.

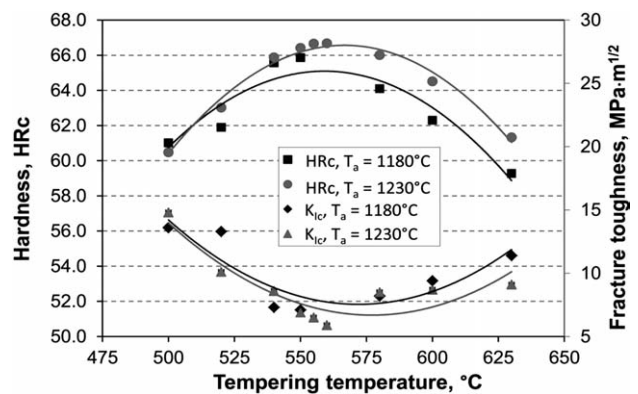


Figure 4: Tempering diagram for the investigated AISI M2 high-speed steel

Slika 4: Diagram popuščanja pri preiskovanem hitrozreznem jeklu AISI M2

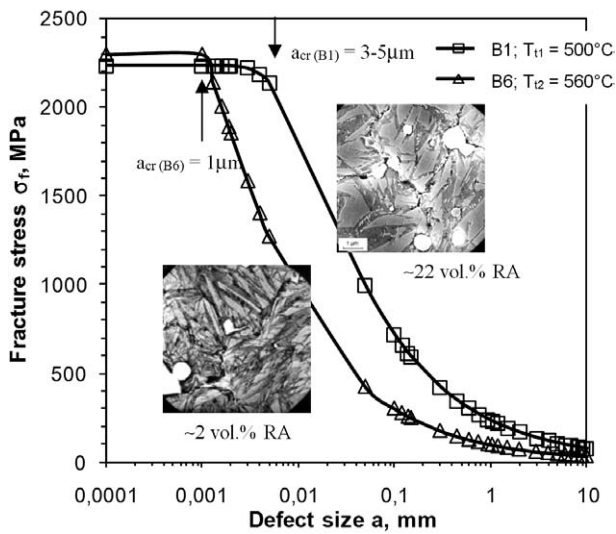


Figure 5: Example of the calculated fracture stress
Slika 5: Primer izračunane napetosti loma

Based on the fracture toughness K_{Ic} and the ultimate tensile stress σ_u , estimated from the Rockwell-C hardness, the fracture stress σ_f can be calculated.³⁷ A reduction in the fracture stress is observed, when the defect size, represented by carbides and carbide clusters, exceeds a critical value.¹⁰ This gives us a tool to estimate the critical defect size in vacuum heat-treated high-speed steel depending on the austenitizing and tempering temperatures. For example, in the case of an austenitizing temperature of 1230 °C and a tempering temperature of 500 °C the critical defect size is in the range of 3–5 μm , while it is reduced to about 1 μm for a tempering temperature of 560 °C, at the same time showing a faster drop in the fracture stress with the defect size (Figure 5).

4.3 Bending and compression strength

The results of the bending and compression tests, performed on 6 groups of specimens (A1, A4, A9, B1, B4 and B9) are shown in Figures 6 and 7. The bending strength of the investigated high-speed steel is increasing for both austenitizing temperatures as the tempering temperature gets higher. In the case of an austenitizing temperature of 1180 °C the bending yield strength σ_{yB} and the bending strength σ_B reached maximum values of ≈ 4000 MPa and ≈ 4150 MPa at the highest tempering temperature of 630°C. By increasing the austenitizing temperature to 1230 °C the bending yield strength and the bending strength are reduced by about 15 %, as shown in Figure 6.

The compressive strength of the vacuum heat-treated high-speed steel shows the same dependency on the tempering temperature as displayed by the Rockwell-C hardness, with the peak values ($\sigma_{yC} \approx 3000$ MPa, $\sigma_C \approx 3600$ MPa) reached at the intermediate tempering temperature of 550 °C. However, no noticeable difference in the compressive strength was observed between

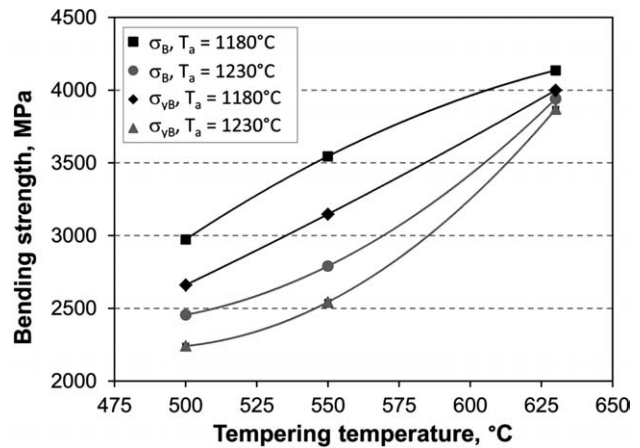


Figure 6: Bending-test results for vacuum heat-treated AISI M2 high-speed steel

Slika 6: Rezultati upogibnega preizkusa za vakuumsko toplotno obdelano hitroreznno jeklo AISI M2

the two austenitizing temperatures used (Figure 7). On the other hand, the strain-hardening exponent, indicating the ductility of the material, shows a steep decrease with increasing tempering temperature, while an increase in the austenitizing temperature has the opposite effect, as shown in Figure 7. The strain hardening exponent of the investigated high-speed steel, austenitized from 1180 °C, was reduced from 0.18 down to 0.04 as the tempering temperature increased from 500 °C to 630 °C. When using a higher austenitizing temperature of 1230 °C the strain-hardening exponent also increased, indicating better ductility. For under-tempered specimens ($T_{temp} = 500$ °C) it increased to 0.31 and for specimens tempered at 630 °C to 0.07 (Figure 7).

4.4 High-speed machinability and grindability

In order to evaluate the high-speed machinability behaviour of vacuum heat-treated high-speed steel investigation of cutting inserts was carried out. In the

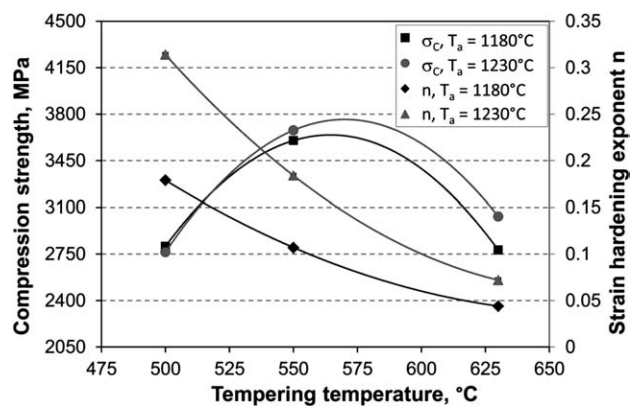


Figure 7: Compression test results for vacuum heat-treated AISI M2 high-speed steel; curves for σ_c are obtained with quadratic regression

Slika 7: Rezultati tlačnih preizkusov vakuumsko toplotno obdelanega hitroreznega jekla AISI M2; krivulje σ_c so dobljene s kvadratno regresijo

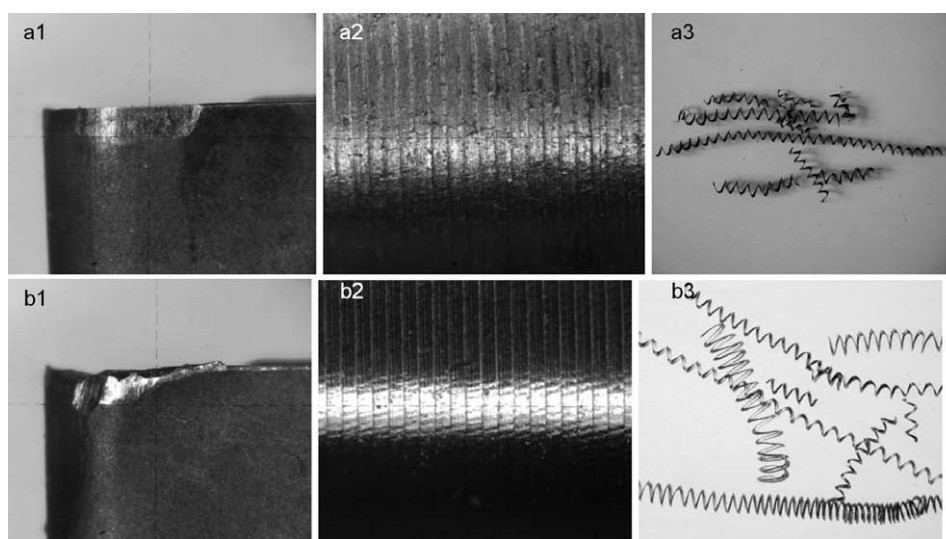


Figure 8: High-speed machinability test results for: a) specimen A1 ($t = 8.5$ mm) and b) specimen A4 ($t = 9.2$ min); 1) edge of the cutting insert at the end of the test, 2) machined surfaces and 3) associated chips

Slika 8: Rezultati preizkusa obdelovalnosti z veliko hitrostjo za: a) vzorec A1 ($t = 8,5$ mm) in b) vzorec A4 ($t = 9,2$ min); 1) rob rezalne ploščice na koncu preizkusa, 2) obdelana površina in 3) pripadajoči ostružki

absence of a systematic observation of the cutting inserts as a function of time the observed difference in the appearance of the cutting inserts at the end of the tool life was used to draw qualitative information. In most cases a stable evolution of the wear along both the rake and flank surface was observed, being a result of one or a combination of the following modes; namely, abrasive wear along with progressive micro-chipping, notching, localized chipping and final destruction of the edge. A comparison of the cutting inserts' worn edge used to machine specimens tempered at 500 °C (A1) and 550 °C (A4), together with the machined surface and the corresponding chips is shown in **Figure 8**. In the case of a worse machinability tendency for notch formation and adhesion of the work material to the cutting insert was evident. However, when the work material adhesion was postponed, as was the case for the specimens tempered at 550 °C (**Figure 8b**), the tool life was sufficiently prolonged (≈ 10 %). Indirect evidence of better machinability also comes from the appearance of the chips, which for the higher tempering temperature become more continuous, longer and smoother (**Figure 8b**).

From the investigation performed it can be concluded that the high-speed machining of vacuum heat-treated high-speed steel poses no technical problem. However, it was observed that even at a comparable hardness level, the increase in the carbide content observed for the lower austenitizing temperature contributed to a deterioration in the machinability of high-speed steel. At this point it should be pointed out that proper cutting inserts (material and micro-geometry) and cutting conditions have to be selected to achieve the optimal tool life.

In spite of the fact that normally the G-ratio of a grinding wheel is used to measure the grinding efficiency, our focus was on the quality of the ground

surface. Therefore, the surface roughness of the 4-point bending-test specimens (A1, A4, A9, B1, B4 and B9) was analysed after grinding. The results are summarized in **Table 2**.

Table 2: Surface roughness after high-speed centreless grinding

Tabela 2: Hrapavost površine po "centreless" brušenju z veliko hitrostjo

Roughness	4-point bending test specimen					
	A1	A4	A9	B1	B4	B9
$R_a/\mu\text{m}$	0.21	0.18	0.19	0.21	0.20	0.18
$R_{\text{max}}/\mu\text{m}$	1.88	1.62	1.82	1.85	1.82	1.81

For the selected high-speed centreless grinding parameters and specimens austenitized from 1180 °C (group A) the smoothest surface with a minimum average roughness of 0.18 μm was reached in the case of specimen A4, tempered at 550 °C. In the case of specimens austenitized from 1230 °C the surface quality was found to improve with an increased tempering temperature, as shown in **Table 2**. In terms of the roughness level, no noticeable difference was observed between the two austenitizing temperatures used. However, SEM microscopy of the surface after high-speed machining and centreless grinding revealed that for a higher austenitizing temperature (group B) the undissolved eutectic carbide particles were pulled out, which was not the case for group A specimens, austenitized from 1180 °C.

5 DISCUSSION

The properties required from the tool and high-speed steels greatly depend on the application and the process the tool will be used for. In some instances the wear resistance is the main concern, requiring a high hardness

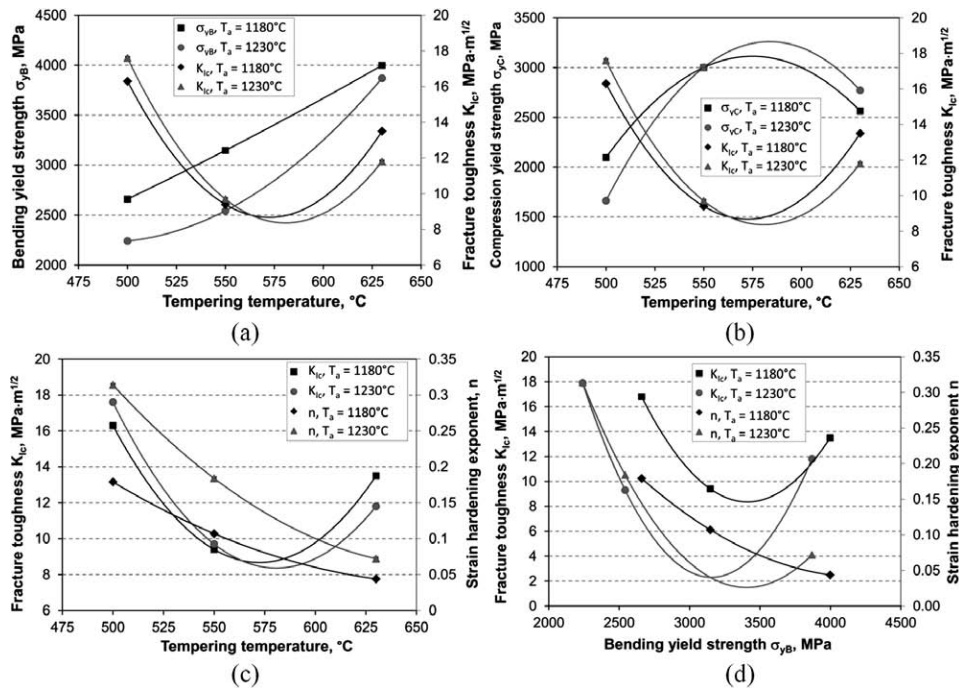


Figure 9: Examples of tempering diagrams combining different properties required from tool material (a–c); a) bending yield strength and fracture toughness, b) compression yield strength and fracture toughness, c) fracture toughness and strain hardening exponent, and d) diagram combining fracture toughness, strain hardening exponent and bending yield strength

Slika 9: Primeri popuščnih diagramov, ki kombinirajo različne lastnosti, zahtevane od materiala orodja (a–c); a) meja tečenja pri upogibu in lomna žilavost, b) meja tečenja pri tlaku in lomna žilavost, c) lomna žilavost in eksponent napetostnega utrjevanja in d) diagram, ki kombinira lomno žilavost, eksponent napetostnega utrjevanja in mejo tečenja pri upogibu

at sufficient fracture toughness, while in others the fatigue properties and the resistance to crack propagation are more important, demanding a high fracture toughness and bending strength. Thus, the combination of different tool properties becomes important and should be optimized for a specific tool through proper vacuum heat-treatment. Besides tempering diagrams displaying the fracture toughness and hardness as a function of the austenitizing and tempering temperatures (Figure 4) diagrams combining other tool and high-speed steel properties can also be prepared in order to relate the properties of the material to its performance. For example, when looking for toughness, a properties combination of fracture toughness and bending or compression yield strength should be used (Figures 9a and 9b), and for ductility, a combination of fracture toughness and strain hardening exponent should be used (Figure 9c). However, an accurate comparison and correlation of different material properties, as exemplified in Figure 9d, combining the fracture toughness, the strain hardening exponent and the bending yield strength is only possible when different specimens are vacuum heat-treated under identical conditions, not only in terms of temperature and time, but more importantly in terms of heat transfer and microstructure uniformity.

As already mentioned, due to the axial symmetry and uniform heat transfer the K_{Ic} -test specimens are particularly suitable for studying the influence of vacuum heat-treatment parameters on the microstructure of

metallic materials and consequently on their properties. Since different test specimens can be made from the same K_{Ic} -test specimen, a proper correlation between the different material properties can also be carried out and statistically analysed if using relevant number of K_{Ic} -test specimens.

After measuring the fracture toughness, using the K_{Ic} -test specimen, two halves of the test sample are obtained, as shown in Figure 10. Both parts can be used for a Rockwell-C or Vickers hardness measurement. Then, from one of the halves a metallographic specimen ($\phi 10\text{ mm} \times 6\text{ mm}$) is cut for analysis of the fractured surface and the microstructure just below the fracture.

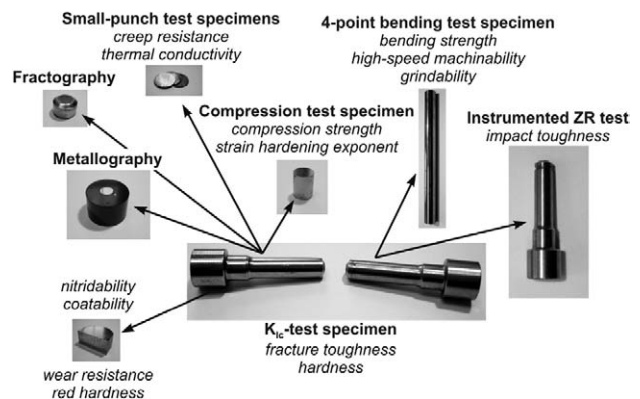


Figure 10: Versatility of K_{Ic} -test specimen
Slika 10: Vsestranskost K_{Ic} -preizkušanca

From the same part of the K_{Ic} -test specimen, also the compression test specimen ($\phi 10$ mm \times 12.5 mm) is cut and used to determine the compressive strength, the compressive yield strength and the strain-hardening exponent, correlating with the ductility of the steels. The remaining can be used for an evaluation of the creep resistance using the small-punch method ($\phi 8$ mm \times 0.5 mm), the thermal conductivity, the wear resistance or for an assessment of technological properties such as nitridability, suitability for hard coating deposition, etc. The other half of the fractured K_{Ic} -test specimen is used to manufacture a 4-point bending test specimen ($\phi 5$ mm \times 60 mm) for an assessment of the bending strength. During the manufacturing the high-speed machinability and grindability in the hardened and tempered conditions can also be evaluated. If bending properties are not required a modified specimen with a circumferential notch ($r = 10$ mm, $z = 1$ mm) for instrumented impact ZR testing²⁵ can be prepared. An instrumented impact test provides the initial and maximum fracture force, the total fracture time, the time to maximum fracture force, the force-time diagram and the work used. The main advantage of such an impact test lies in the possibility to obtain a single fracture without shattering. This allows further examination of the fractured surface, including X-ray diffraction.

6 CONCLUSIONS

In the present paper the multi-functional K_{Ic} -test specimen is presented. The idea is to minimize the costs for tool and high-speed steel characterization. Due to the fact that none of the standard tests alone is capable of describing all the relevant properties, more than one test is required. Besides this, the test results need to be related to the service behaviour of the tool and high-speed steels.

With the use of a K_{Ic} -test specimen, it is possible to simultaneously assess basic properties such as hardness, fracture toughness, bend and compressive strength etc., which can be directly correlated to the vacuum heat-treatment parameters and microstructure obtained. In this way the heat treatment of the tool and high-speed steels can be optimized for a specific application. The other properties such as wear and creep resistance, machinability, grindability, nitridability, hard-coatings adhesion etc., can be determined and correlated to the microstructure as well as between each other.

As a result of the relatively simple and economical manufacturing of the axially symmetric K_{Ic} -test specimen, a sufficient number of specimens (10–20) for statistical analyses can be produced, allowing an accurate and reliable evaluation of the tool and high-speed steel properties.

7 REFERENCES

¹ R. Ebara, K. Kubota, Failure analysis of hot forging dies for automotive components, *Eng. Fail. Anal.*, 15 (2008), 881–893

- ² B. A. Behrens, E. Doege, S. Reinsch, K. Telkamp, H. Daehndel, A. Specker, Precision forging processes for high-duty automotive components, *J. Mater. Process. Technol.*, 185 (2007), 139–146
- ³ M. Bayramoglu, H. Polat, N. Geren, Cost and performance evaluation of different surface treated dies for hot forging process, *J. Mater. Process. Technol.*, 205 (2008), 394–403
- ⁴ L. Lavtar, T. Muhic, G. Kugler, M. Tercelj, Analysis of the main types of damage on a pair of industrial dies for hot forging car steering mechanisms, *Eng. Fail. Anal.*, 18 (2011), 1143–1152
- ⁵ R. Seidel, H. Luig, Friction and wear processes in hot die forging, *Proceedings of International Conference on Tooling Materials, Interlaken, Switzerland, 1992*, 467–480
- ⁶ O. Barrau, C. Boher, C. Vergne, F. Rezaei-Aria, Investigations on friction and wear mechanisms of hot forging tool steels, *Proceedings of 6th International Tooling Conference, Karlstad, Sweden, 2002*, 81–94
- ⁷ K. H. Schwalbe, On the influence of microstructure on crack propagation mechanisms and fracture toughness of metallic materials, *Eng. Fract. Mech.*, 9 (1977), 795–832
- ⁸ H. Jespersen, Toughness of tool steels, *Proceedings of 5th International Conference on Tooling, Leoben, Austria, 1999*, 93–102
- ⁹ U. Krupp, *Fatigue Crack Propagation in Metals and Alloys: Microstructural Aspects and Modelling Concepts*, John Wiley & Sons, Weinheim 2007
- ¹⁰ V. Leskovsek, B. Sustarsic, G. Jutrisa, The influence of austenitizing and tempering temperature on the hardness and fracture toughness of hot-worked H11 tool steel, *J. Mater. Process. Technol.*, 178 (2006), 328–334
- ¹¹ V. Leskovsek, B. Ule, B. Liscic, Relations between fracture toughness, hardness and microstructure of vacuum heat-treated high-speed steel, *J. Mater. Process. Technol.*, 127 (2002), 298–308
- ¹² R. Ebner, H. Leitner, F. Jeglitsch, D. Caliskanoglu, Methods of property oriented tool steel design, *Proceedings of 5th International Conference on Tooling, Leoben, Austria, 1999*, 3–24
- ¹³ M. Janssen, J. Zuidema, R. J. H. Wanhill, *Fracture Mechanics*, 2nd ed., Delft University Press, Delft, Netherlands 2002
- ¹⁴ ASTM E399-90: Standard Test Method for Plane-Strain Fracture Toughness of Metallic Materials, 1997
- ¹⁵ ASTM E1820-11: Standard Test Method for Measurement of Fracture Toughness, 2011
- ¹⁶ V. Leskovsek, B. Podgornik, Vacuum heat treatment, deep cryogenic treatment and simultaneous pulse plasma nitriding and tempering of P/M S390MC steel, *Mater. Sci. Eng., A* 531 (2012), 119–129
- ¹⁷ W. Chang, Applying similarity methods to fracture mechanics measurement of fracture toughness K_{Ic} , KQ values by small-scale single specimen, *Eng. Fract. Mech.*, 31 (1988), 807–816
- ¹⁸ W. Chang, An improvement of applying similarity methods to fracture mechanics-measurement of fracture toughness K_{Ic} , KQ values by smallscale single specimen, *Eng. Fract. Mech.*, 36 (1990), 313–320
- ¹⁹ B. Ule, V. Leskovsek, B. Tuma, Estimation of plain strain fracture toughness of AISI M2 steel from precracked round-bar specimens, *Eng. Fract. Mech.*, 65 (2000), 559–572
- ²⁰ V. Leskovsek, B. Ule, A. Rodic, Development of a modified method for determining fracture toughness of HSS with non-standard cylindrical round-notched tension specimens, *Met. Alloys Technol.*, 27 (1993), 195–204
- ²¹ S. Wei, Z. Tingshi, G. Daxing, L. Dunkang, L. Poliang, Q. Xiaoyun, Fracture toughness measurement by cylindrical specimen with ring-shaped crack, *Eng. Fract. Mech.*, 16 (1982), 69–92
- ²² H. F. Bueckner, Discussion on "Stress analysis of cracks" by P. C. Paris, G. C. Sih, *ASTM-STP*, 381 (1965), 82
- ²³ H. F. Fischmeister, L. R. Olson, *Cutting Tool Materials*, Proceedings of International Conference on Cutting Tool Materials, Ft. Mitchell, Kentucky, USA, 1980, 111–118
- ²⁴ ASTM E290-09: Standard Test Methods for Bend Testing of Material for Ductility, 2009
- ²⁵ G. Hoyle, *High Speed Steels*, Butterworths & Co., London 1988

- ²⁶ ASTM E9-09: Standard Test Methods of Compression Testing of Metallic Materials at Room Temperature, 2009
- ²⁷ ASTM E209-00: Standard Practice for Compression Tests of Metallic Materials at Elevated Temperatures with Conventional or Rapid Heating Rates and Strain Rates, 2010
- ²⁸ J. Kopac, V. Leskovsek, Minimizing of machining effect on HSS structure characteristics, Proceedings of 7th international tooling conference – Tooling materials and their applications from research to market, Torino, Italy, 2006, 303–311
- ²⁹ J. R. Koelsch, High-speed machining: A strategic weapon, Machine Shop Guide, November 2001
- ³⁰ L. P. Tarasov, Some Metallurgical Aspects of Grinding, in: Machining Theory and Practice, American Society for Metals, Metal Park, Ohio, 1950, 409–464
- ³¹ L. P. Tarasov, Grindability of Tool Steels, Trans. Amer. Soc. Metals, 43 (1951), 1144–1151
- ³² J. Badger, Grindability of Conventionally Produced and Powder-Metallurgy High-Speed Steel, Annals of the CIRP, 56 (2007), 353–356
- ³³ W. König, J. Messer, Influence of the Composition and Structure of Steels on Grinding Process, Annals of the CIRP, 30 (1981), 547–552
- ³⁴ K. Kishi, Y. Ichida, S. Marumo, Effects of Grain Refining of Carbides on the Grindability of High-Vanadium High-Speed Steels, Proceedings of the 25th Japan Congress of Materials Research, Tokyo, Japan, 1982, 171–176
- ³⁵ B. Šuštaršič, Composite high speed steel with solid lubricant, Ph. D. thesis, Ljubljana, 2000
- ³⁶ H. Chandrasekaran, H. Izadi, O. Johansson, Temperature and thermal damage during grinding of some tool steels, Proceedings of 5th International conference on tooling, Leoben Austria, 1999, 539–549
- ³⁷ S. Karagoz, H. Fischmeister, Microstructure and toughness in high-speed tool steels – the influence of hot reduction and austenitization temperature, Steel research, 58 (1987), 353–361